JOURNAL OF MATERIALS SCIENCE 29 (1994) 4742–4749

Al–V–graphite interface reactions: an XAFS study of the reactions in a composite interface system

E. V. BARRERA, C. USLU
Department of Mechanical Engineering and Materials Science, Rice University, Houston, TX 77251, USA

The high temperature reaction properties of a metal matrix composite interface have been observed in this research by X-ray reflectivity and X-ray absorption fine structure (XAFS) coupled to Auger electron spectroscopy (AES). This study was taken from the vantage point of the vanadium diffusion barrier interfacial layer in a model aluminum–graphite metal–matrix laminate composite. The interfacial couple of aluminum and vanadium was analysed to ascertain the reaction species at temperatures between 200 and 350 °C. X-ray reflectivity and glancing angle XAFS showed that the initial Al–V reaction occurred at 325 °C where the aluminum-rich intermetallic Al_3V formed. Small angle XAFS was used to analyse the higher temperature interfacial changes in the temperature range of 300–500 °C. Further interactions occurred at 500 °C, where interdiffusion of Al, C and O occurred leading to phase formation of the vanadium, dependent on the graphite basal plane orientation. AES, used to determine the initial compositions and those resulting from the high temperature heat treatments, complemented the XAFS results.

1. Introduction

A model laminate aluminum matrix–graphite reinforcement system with a high purity metal vanadium diffusion barrier layer was designed to investigate the reaction processes at the interfacial region as a function of increasing temperature. The objectives were to observe the as-formed interfacial conditions and to determine the effects of elevated temperature on this region. An Al–graphite system was of interest here, since many metal–matrix composites involve these materials in combination while requiring their interaction in the form of aluminum carbide, Al_4C_3, to be minimized. Vanadium was considered for the interfacial layer since it has a high melting temperature (T_m = 1890 °C) compared to 660 °C for aluminum, and a density of 6.11 $g\,cm^{-3}$ compared to 2.70 $g\,cm^{-3}$ for aluminum [1]. Its high melting temperature suggests refractory properties. Of equal importance are the possible reaction products that could form *in situ* which would lead to a decrease in the interdiffusion of aluminum and carbon. Likely phases that could form include; the aluminum-rich intermetallic Al_3V, with a melting point of 1362 °C and a density of 3.34 $g\,cm^{-3}$, vanadium oxides of V_2O_5 and VO_2 which would form in the presence of oxygen, have melting points of 690 and 1967 °C with densities of 3.36 and 4.34 $g\,cm^{-3}$, respectively, and vanadium carbide, VC, which has a melting point of 2810 °C and a density of 5.77 $g\,cm^{-3}$.

Vanadium does not have the low density of TiB_2 (4.5 $g\,cm^{-3}$), commonly found in numerous composite systems as a reinforcement coating, yet was considered here as an alternative and studied because previous investigations of the Al/V/graphite system did not completely discern the reactiveness of the interface [2, 3]. The maximum operating temperature of a composite system of this type would be approximately half T_m of the aluminum matrix, a temperature at which creep properties would have to be considered. Temperatures of up to 500 °C were considered here for purposes of *in situ* interface processing.

In this research the chemical reactivity of a composite interface region was analysed extensively by means of X-ray absorption fine structure (XAFS) spectroscopy. The specific approaches included: X-ray reflectivity, glancing angle XAFS, small angle XAFS and transmission XAFS. Auger electron spectroscopy (AES) consisting of select point analysis and depth profiling was coupled to the XAFS to further analyse the interfacial region. XAFS probed the interface from the standpoint of the vanadium layer and the changes that occurred to it. In this manner the initial conditions of the vanadium in the interface of the aluminum/graphite composite system could be compared to the conditions after high temperature exposure. The AES data would serve to verify the as-formed conditions and the effects of the high temperature (500 °C) heat treatments. X-ray reflectivity measurements yielded a density profile with depth, providing nanometre depth resolution and was sensitive to elemental concentrations as low as 1% [4]. From the density profile, local interface roughness, layer thicknesses and elemental concentrations were determined. XAFS experiments conducted at glancing angles to

0022–2461 © *1994 Chapman & Hall*

the sample surface provided X-ray penetration through the aluminum overlayer but only into the Al–V interface. Structural information, such as atomic distances and the near neighbour atom type could be determined. Extensive data interpretation could also determine the number of near neighbours and atom placement [5]. Glancing angle XAFS was useful to determine the phases which were present at the interface. Recent work by Heald and Barrera [6] showed the utility of X-ray reflectivity combined with glancing angle XAFS to investigate Al/Ni interfaces. In addition, with the incoming X-rays positioned at angles up to 5° with the sample, small angle XAFS lead to phase determination and could observe changes to the vanadium interfacial layer. Transmission XAFS, where a portion of the X-ray beam passed through the specimen, was useful for powder and thin foil samples and was used to characterize the standard materials used in this research.

In this paper, the data obtained from XAFS will be explained as to its use in characterizing the conditions of the vanadium layer in the aluminum/graphite model composite system following various elevated temperature heat treatments. The ability to analyse the interface from a structural and nanometre vantage point will be highlighted. The ability to observe and, in effect, control *in situ* interfacial processes will also be of primary interest. The reactive nature of this model composite system will provide significant insight into other composite systems where interface reactivity is a concern.

2. Sample preparation and experimental procedures

2.1. Sample preparation

X-ray techniques and synchrotron X-ray techniques used to gain structural information are notably shallow probing techniques. XAFS, as well as X-ray diffraction (XRD) probe micrometre to submicrometre distances as compared to millimetre or less distances probed by neutron techniques [7]. However, both X-ray diffraction and XAFS have higher depth sensitivity compared to neutron diffraction and since near interface properties are of interest where specific properties associated with the interface layer are desired, the XAFS approach supersedes both neutron and X-ray diffraction since it is an atom specific technique. To accomplish this research four types of samples were used; Al on V on float glass, Al on V on a silicon wafer, and composites of Al on V on graphite with the carbon basal planes parallel and perpendicular to the surface of the sample. The samples will be labelled as follows: A/V/G, Al/V/glass; A/V/S, Al/V/silicon; A/V/PA, composite with carbon basal planes parallel to the sample surface; A/V/PP, composite with the carbon basal planes perpendicular to the sample surface.

Layering of Al and V were accomplished by thin film deposition. The float glass substrates were prepared by cleaning in boiling isopropyl alcohol followed by air drying before loading in the ultra high vacuum chamber. The surface of the Si wafers were prepared by ultrasonic cleaning in acetone and methanol and were allowed to dry in air. Pyrolytic graphite was cut using a diamond wafering saw with methanol rinsing. The surfaces were polished and adhesive tape was used to pull off the top layer to expose a clean surface before loading in the vacuum chamber. The graphite was thought to have residual moisture at the time of loading. The vacuum chamber was baked to $\sim 150\,°C$ for 24 h prior to deposition. The amount of moisture removed from the graphite during baking was not determined.

High purity aluminum (99.999%) and vanadium (99.9%) were used in this research and were resistively evaporated from tungsten boats. The sources were thoroughly degassed prior to sample deposition. The vacuum before deposition was $8.0–10.7 \times 10^{-8}$ Pa and during deposition was $2.7–6.7 \times 10^{-7}$ Pa. Deposition rates were 6 nm min^{-1}. The substrates were cooled to a low temperature ($-40\,°C$) using liquid nitrogen. The sample temperature increased $\sim 15°$ during deposition. In this research the substrates were kept at low temperatures to reduce the possibility of reaction during deposition and to eliminate roughening of the interfaces due to mixing. The sample processing was conducted with the utmost care to prevent oxygen and carbon contamination. Oxygen is recognized to alter the interfacial reactions [6]. Deposition on graphite was in the same manner as that for the float glass and Si wafer substrates. Thicknesses were measured using an oscillating quartz crystal monitor which had high relative accuracy. The thicknesses of the aluminum and vanadium layers were 50 nm each, in all cases.

Compositions and contamination levels were analysed using AES on the A/V/S sample. The A/V/S sample was used rather than the A/V/G since the glass substrate would charge when exposed to the electron beam. Further AES analysis was conducted on the A/V/PA and A/V/PP samples as-deposited and after the high temperature heat treatments. AES analysis consisted of select point analysis of the sample surface followed by depth profiling during inert gas (argon) sputtering using a Physical Electronics 590. Typical scan and profiling parameters included: beam voltage, 3 kV; beam current, 150 nA; modulation voltage, 3 eV for a photon energy less than 600 eV and 6 eV for a photon energy greater than 600 eV; multiplier voltage, 1050 V; a time constant of 0.3; and a scan rate of 5 eV s^{-1}. During the depth profiles, the sputtering was stopped intermittently to conduct further select point analysis at that depth. The depth profiles were repeated to conform uniformity of the layers.

Samples of 99.99% pure vanadium foil, and powders of V_2O_5, VC and Al_3Ti were used as structure standards for comparison with the composite samples for XAFS analysis. The Al_3Ti was processed into a powder by melt spinning followed by grinding by mortar and pestle, the structure was confirmed by XRD [8]. The Al_3Ti served as a standard for Al_3V on the basis that elements with similar atomic number, Z (for Ti $Z = 22$, for V $Z = 23$), produce similar XAFS when the structure is the same (in this case tetragonal).

It will be evident that the structural data of XAFS for the samples of interest can easily be compared to the structural information of standard samples [5]. The vanadium foil was mounted on an aluminum holder for transmission XAFS experiments. The powders were applied on a low X-ray absorbing adhesive tape, cut into pieces and layered to an appropriate thickness to conduct transmission XAFS experiments.

2.2. XAFS measurements

XAFS experiments were conducted using Beamline X-11A at the National Synchrotron Light Source (NSLS) at Brookhaven National Laboratory (BNL) with a ring energy of 2.5 GeV and currents of 100–200 mA. A double crystal Si (1 1 1) monochromator was used with an energy resolution of 1.5 eV at the V K-edge. The monochromator was detuned 20–30% to reduce the harmonic content of the incident X-ray beam to less than 0.1%. Calibration of the monochromator was initially set by running a Cu K-edge (8989 eV) scan, followed by an XAFS scan of the V K-edge (5464 eV). Table I shows the experiments that were conducted and the samples analysed. X-ray reflectivity and glancing angle XAFS were conducted on the A/V/G samples using the experimental set-up shown in Fig. 1. The slits were used to size down the X-ray incident beam, I_0 identifies the ion chamber which measures the intensity of the incident X-rays, θ is the sample angle made by tilting the sample stage away from the horizontal plane. Increasing θ meant deeper penetration of the X-rays into the sample. I_f identifies the fluorescence ion chamber used to measure the fluorescence signal to yield I_f/I_0 data. I_r identifies the ion chamber used to measure the intensity of reflected X-ray beam used to generate I_r/I_0 data, or for transmission experiments where ln (I_0/I) is obtained.

X-ray reflectivity experiments were conducted by setting the X-rays at a single energy (wavelength) and conducting a motor scan of the sample stage. Scans at −300 eV to the V K-edge energy and +300 eV to the same edge were run and made up one set of data for a sample [9]. Following heat treatment each sample was analysed in the same manner. Fig. 2 shows the experimental reflectivity data for the room temperature (RT) sample (Fig. 2a) and the 325 °C sample where the effects of the heat treatments are seen (Fig. 2b). At small θ, the X-rays were almost totally reflected from the surface and as the angle was increased the X-rays were absorbed. The frequency and amplitude of the oscillations seen after the first minimum contributed to the determination of the layer thicknesses and roughness. The dotted lines represent fitted curves which will be discussed later. Glancing angle XAFS were run following the reflectivity scans with the sample angle fixed close to the first minimum on the reflectivity scans for interface analysis and at small angles where bulk properties were observed. The small angle scans also served as a method to check the calibration of the edge energy. To run the XAFS scan, the sample position was fixed and the monochromator was scanned to yield a scan in energy.

Transmission V K-edge XAFS was run on samples of vanadium foil, V_2O_5, VC and Al_3Ti (Ti K-edge), where I_r was used to measure the transmitted signal rather than reflected signal. Small angle XAFS were run on the A/V/PA and A/V/PP specimens. Fig. 3 shows the small angle XAFS experimental data for a Al/V/graphite specimen. The pre-edge, edge background and XAFS regions of the data are as labelled. In these experiments the sample was positioned at a 5° tilt with the incident X-ray beam and I_f/I_0 data versus photon energy was acquired. The angle was chosen where the X-rays penetrated the Al and V layers and a portion of the graphite substrate.

TABLE I Experiments to ascertain the reactions in an Al/V/graphite system

Sample	Experimentation	Temperature (°C)
A/V/G	X-ray reflectivity, glancing angle XAFS	RT, 200, 250, 300, 325, 350
A/V/S	AES	RT
A/V/PA	Small angle XAFS, AES at RT and 500 °C	RT, 300, 350, 400, 450, 500[a]
A/V/PP	Small angle XAFS, AES at RT and 500 °C	RT, 300, 350, 400, 450, 500[a]
V, V_2O_5, VC, Al_3Ti	Transmission XAFS	RT

[a]All heat treatments were for 10 min time periods in flowing argon. The A/V/PA and A/V/PP samples were heat treated a second time at 500 °C following the 10 min treatment, A/V/PA for 20 min and A/V/PP for 30 min.

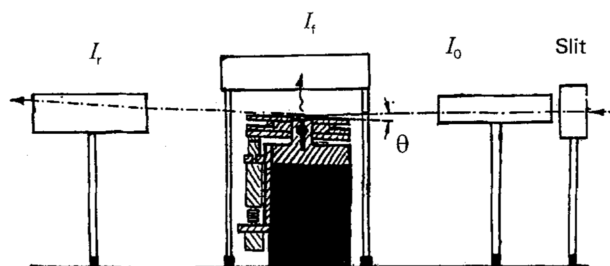

Figure 1 The XAFS experimental set up for X-ray reflectivity, glancing and small angle XAFS.

3. Results and discussion

3.1. The Al–V interface: local interfacial properties

3.1.1. X-ray reflectivity

To obtain local interfacial properties, a density profile was obtained from the reflectivity data. The density profile was extracted by using a least squares fitting procedure [9, 10]. The fitting is shown on Fig. 2 by the dotted curves which were obtained by modelling the RT sample (Fig. 2a) and the 325 °C sample as a series of layers of various thickness, composition and interfacial roughness (Fig. 2b). Generally, the number of layers was kept to a minimum where there was usually an Al oxide overlayer, a pure Al layer, a mixed Al–V layer and a pure metal (V) layer. For cases where the reactions were more extensive, more than one mixed

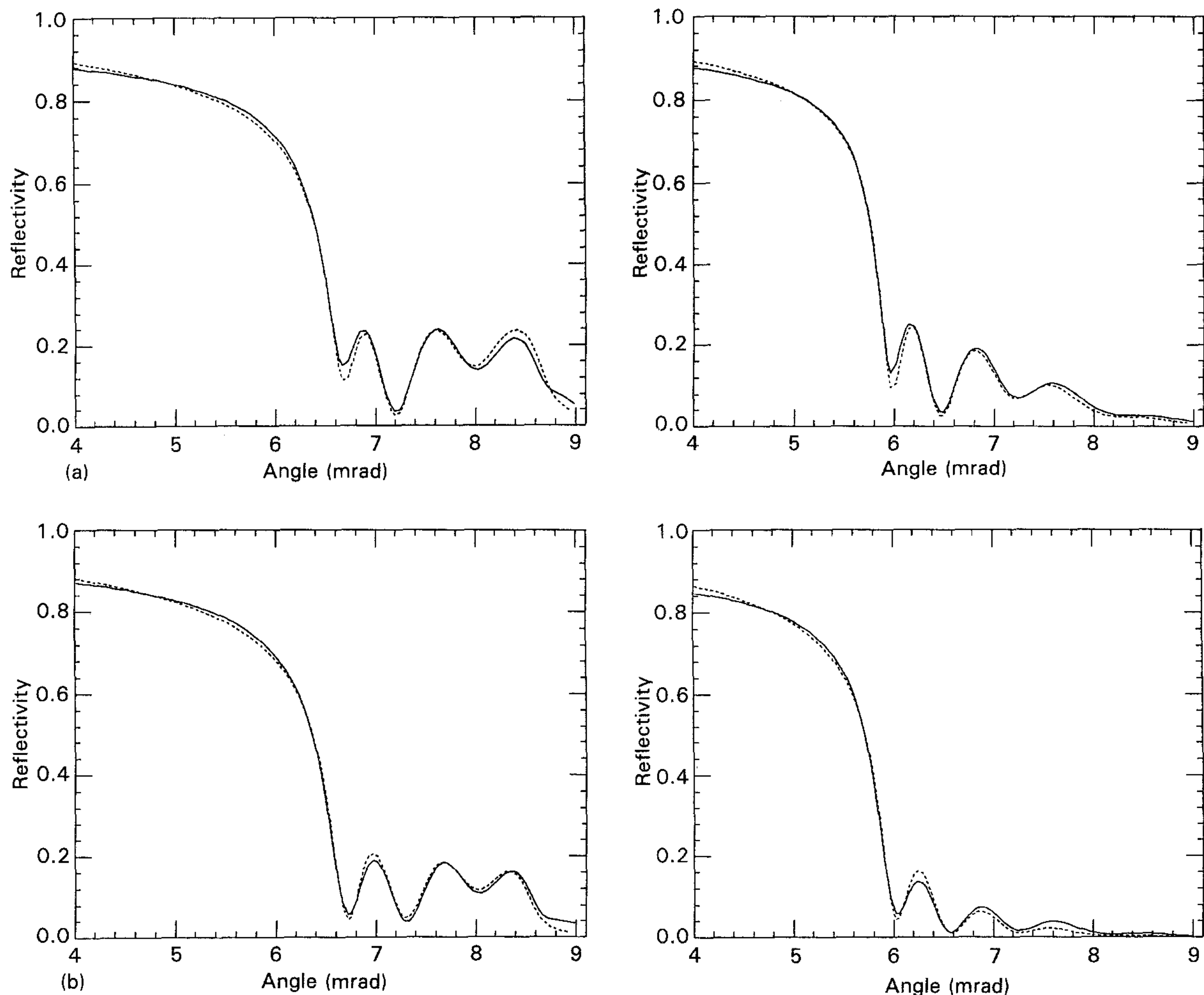

Figure 2 X-ray reflectivity data obtained at 5.16 and 5.76 KeV for A/V/G at (a) RT and (b) 325 °C. The dotted lines are fits of the experimental curves.

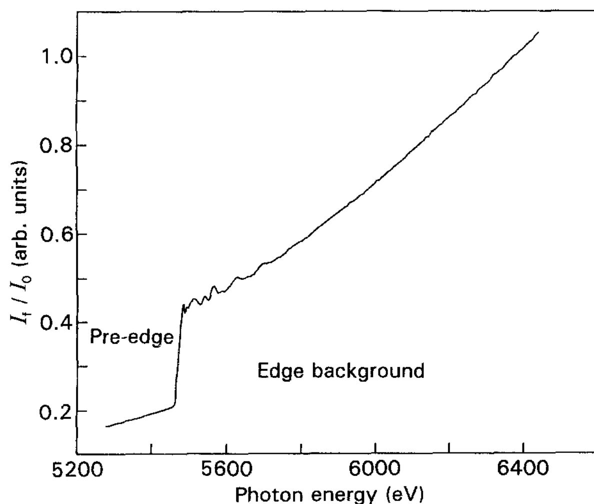

Figure 3 XAFS experimental data of A/V/PA: RT taken with the specimen positioned at a small angle (θ = 5°).

layer was included. From the experimental data the RT specimen remained unchanged until it was heat treated at 325 °C for 10 min. For the cases fitted in this research 10–13 structural parameters were simultaneously fit to the reflectivity data above and below the V K-edge. Having the data from below and above the edge significantly increased the reliability of this analysis technique. The fits were of good quality and the results indicated that an additional mixed layer was needed to accomplish the fit for the 325 °C specimen.

Fig. 4 shows the V depth dependent concentration profiles (density profiles) for the RT and 325 °C specimens. These were obtained by plotting the V concentration for the layers and smoothing the edges using the derived roughness parameters. The profile from the sample was an average composition over approximately 1 cm^2 area of the sample [6]. The RT specimen density profile showed a relatively sharp interface with interfacial mixing of Al and V over roughly 10 nm. Since high temperatures of the V source material had to be reached to deposit the V on the float glass ($\sim$ 1100 °C at $\sim 10^{-5}$ Pa) a relatively rough surface was observed as compared to previous research [6, 9, 10]. Changes in the interface did not occur until a temperature of 325 °C was reached. The profile for the 325 °C specimen changed in that a layer had to be added to the previous two-layer model where the intermediate layer composition did not exceed a value associated with the aluminum-rich intermetallic compound (Al_3V). This provided some evidence of formation of the aluminum-rich intermetallic phase. (Note that the glancing angle XAFS data in the next section lent further insight.)

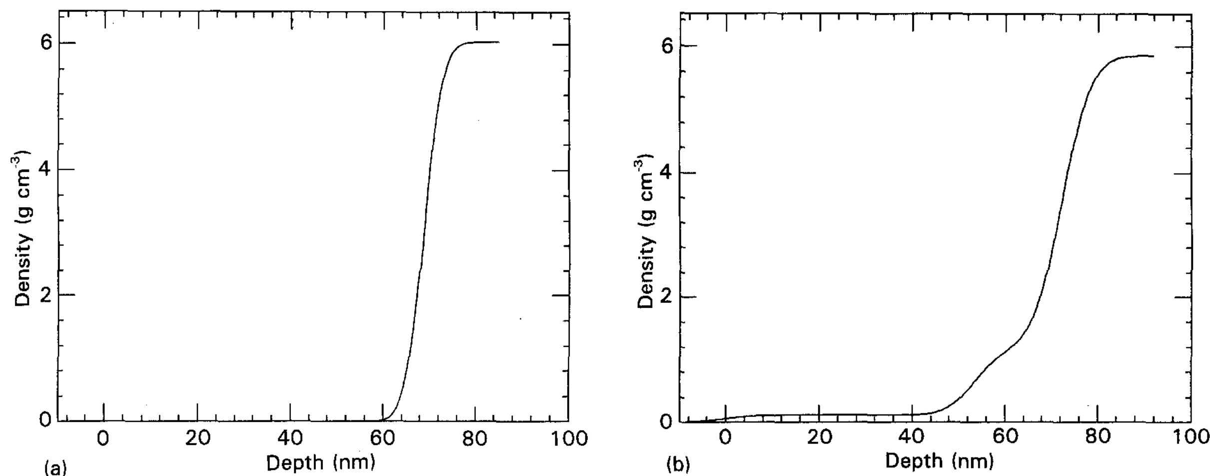

Figure 4 V density profiles obtained for A/V/G: (a) RT and (b) following the 325 °C heat treatment.

3.1.2. Glancing angle and small angle methods

XAFS is best explained by a single scattering expression [5]:

$$\chi(k) = \sum_j \frac{N_j}{R_j^2} A_j(k) e^{-2k^2\sigma_j^2} \sin[2R_j + \phi_j(k)] \quad (1)$$

where $\chi(k)$ is the normalized oscillations as a function of the photoelectron wave vector, k. The atoms were considered to be in shells where each shell ($j = 1, 2, 3\ldots$) had N_j atoms at a distance R_j and a root mean square disorder in the distances, σ_j. $A_j(k)$ and $\phi_j(k)$ are scattering factors which depend on the type of atoms in the shell and are usually calibrated using standard compounds. For the glancing angle XAFS I_f/I_0 was collected where I_f is related to I_0 from absorption data by [10]:

$$\frac{I_f}{I_0} = \left(\frac{\mu_a}{\mu_t}\right)[1 - e^{-\mu_t/x}] \quad (2)$$

where $\mu_a = \mu_A/\sin\theta$, μ_A denotes the absorption of the primary X-rays by only the species of interest, the angle θ is the angle shown in Fig. 1; μ_t is the absorption by all elements in the sample; x is the sample thickness or probe depth. The experimental data is obtained as a function of photon energy and is converted to k-space using the relationship:

$$k = \left[2m_e\left(\frac{E - E_K}{h^2}\right)\right]^{1/2} \quad (3)$$

where m_e is the effective mass of an electron, E is the energy away from the edge energy, E_K, and h is Planck's constant. Two to three scans were taken of each specimen, including the standards and following the various heat treatments seen in Table I. The data was then analysed as a set by keeping the various edge features, energy and k-ranges for analysis the same. To analyse the XAFS the pre-edge and edge background we fitted and subtracted, the XAFS was then multiplied by k to produce $k\chi(k)$ prior to running the Fourier transform, which yielded the magnitude of the transform (M/T) or a distribution of the near neighbours radially out from the central atom. Fig. 5 shows the XAFS for the standard samples used in this research. Fig. 6 shows V XAFS from the A/V/G specimen taken at a small angle and at a glancing angle (interfacial data) following 200, 300 and 350 °C heat treatments. Note that the RT and small angle data are similar to that of V foil, indicating that there was not an extensive reaction between Al and V during deposition. Note also that the data for the 350 °C specimen is significantly different, indicating a reaction had occurred once heat treatments at 325 and 350 °C were conducted. There is a favourable comparison between the reacted samples and Al_3Ti indicating that an aluminum-rich V phase had formed.

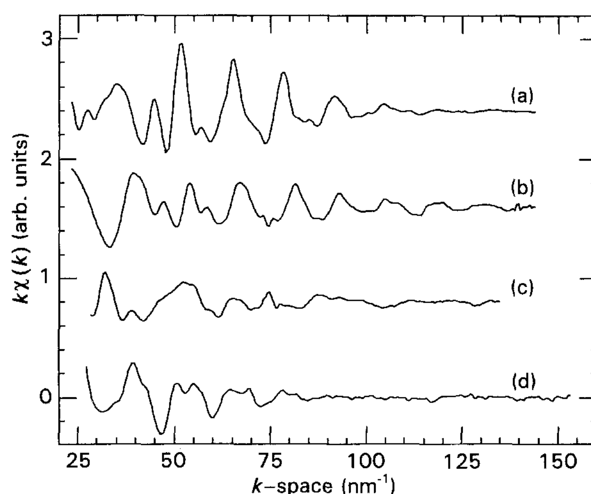

Figure 5 XAFS $k\chi(k)$ for (a) V foil, (b) VC, (c) V_2O_5 and (d) Al_3Ti standard samples used in this research.

3.2. Vanadium in the Al/V/graphite: long range interfacial properties

3.2.1. Small angle XAFS

The Al/V/graphite samples were analysed by small angle ($\theta = 5°$) XAFS. Fig. 7 shows the result of the XAFS analysis for the A/V/PA sample analysed in a fingerprint mode. Shown are XAFS for A/V/PA: RT, 450, 500 for 10 min, and 500 °C for 30 min. Fig 8 shows the XAFS spectra for the A/V/PP: 300, 450, 500 for 10 min, and 500 °C for 40 min. The spectra

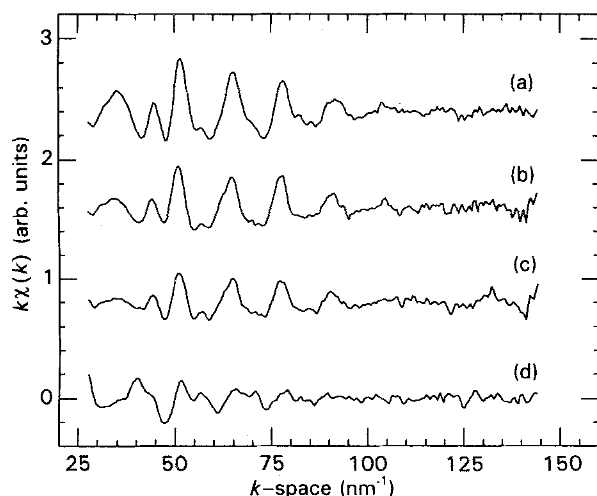

Figure 6 XAFS $k\chi(k)$ for A/V/G: (a) RT specimen taken at a small angle and for (b) 200, (c) 300 and (d) 350 °C for 10 min heat treated cases.

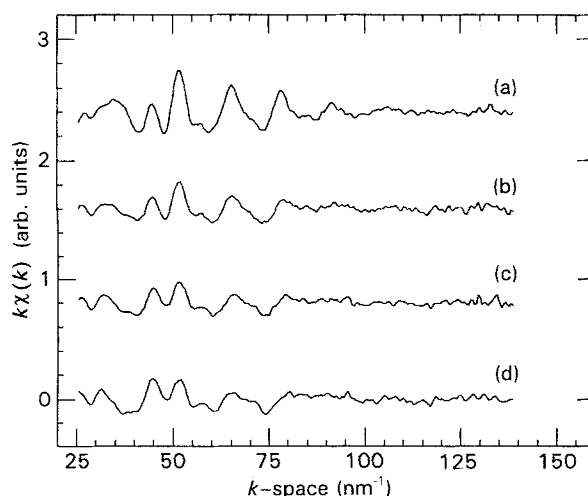

Figure 8 XAFS $k\chi(k)$ for A/V/PP: (a) 300, (b) 450, (c) 500 °C for 10 min, and (d) 500 °C for 40 min.

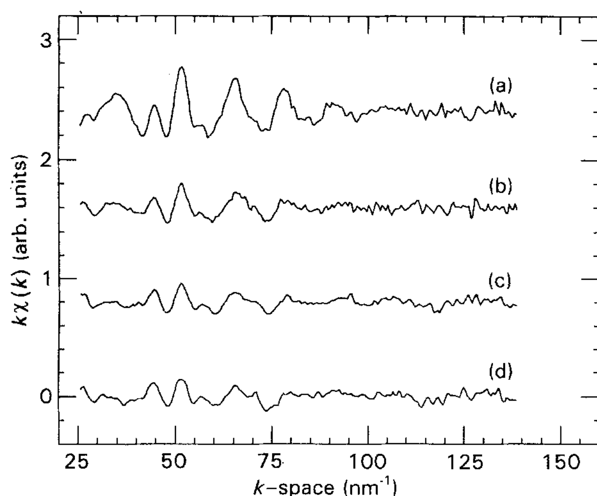

Figure 7 XAFS $k\chi(k)$ for A/V/PA: (a) RT, (b) 450, (c) 500 °C for 10 min, and (d) 500 °C for 30 min.

TABLE II The relationship of the shell distances, *R*, to that of the interatomic spacings (*d*) for vanadium

Shells	*R* (nm)	Interatomic spacings:	*d* (nm)
*R*1	0.234	*d*1	0.262
		*d*2	0.303
*R*2	0.381	*d*3	0.428
*R*3	0.475	*d*4	0.524
		*d*5	0.605

shown are for the specimens where changes were observed due to heat treatment. These results can be discussed considering the features of the various curves. Consider both the $k\chi(k)$ and the M/T for the V foil from a fingerprint standpoint where the $k\chi(k)$ curve is somewhat typical of that of transition metals where the largest oscillations occur between 40 and 50 nm^{-1}. The M/T shows a number of peaks (shells) positioned beyond 0.1 nm from the central V atom indicating shells of atoms. Each shell can have one or more interatomic spacing associated with it. Vanadium is body centred cubic (bcc) where the first two interatomic spacings are 0.262 and 0.303 nm and are separated by 0.041 nm. Using XAFS, these two interatomic spacings will show up in one shell. The third interatomic spacing for V is at 0.428 nm and therefore shows up as the second peak in the M/T. Table II shows a comparison of the measured *R* distances to the interatomic spacings (*d*) for V foil.

As can be observed, the amplitude of the $k\chi(k)$ curves decreased as the specimens were heat treated and small changes at low *k* started to occur for heat treatments above 400 °C. The XAFS were similar up to 400 °C when comparing the A/V/PA and A/V/PP data under the same experimental conditions–changes at low *k* occurred first for the A/V/PP specimen, but the changes were not apparent until heat treatments were conducted at 500 °C, where A/V/PA and A/V/PP were different. It is also evident from both the $k\chi(k)$ and M/T data that V had not fully reacted even when the final heat treatments were completed. Table III shows the changes that occurred in the height of the first peak(s) of the M/T. Note that with extended heat treatment time for the A/V/PP specimen, the height began to increase rather than decrease, indicating a re-ordering by phase formation.

3.2.2. AES analysis

The samples of A/V/S, A/V/PA and A/V/PA heat treated for 30 min, and A/V/PP heat treated for 40 min were argon ion sputtered and analysed by select point analysis at increasing sputtering depths and by depth profiling. The results of the AES analysis can be seen in the select point analysis data where representative layers of the sample are shown. Fig. 9 shows the select point analysis for the A/V/S and the A/V/PP heat treated for 40 min. In all cases the specimens had C and O surface contamination (not shown in Fig. 9) which was not related to the specimen processing. The appropriate AES parameters are shown on the figure. Note that representative spectra are

TABLE III Relative heights of the first shell(s) of the M/T's for the A/V/PA and A/V/PP samples (heights are in arbitrary units)

Temp. (°C)	A/V/PA	A/V/PP
RT	0.225	–
300	0.12	0.128
350	0.11	0.095
400	0.09	0.08
450	0.07	0.07
500	0.05	0.05
500 + [a]	0.045	0.055

[a] 500 + indicates that the specimens were heat treated at 500 °C for a second time to extend the time at this temperature.

shown for the regions pertaining to predominantly; Al overlayer, V interfacial layer and Si or C substrate. Sputtering times are given yet are only relative to the total sputtering time for the particular specimen and for each layer. The evaluation of the various layer regions can only be accomplished by comparing the depth profiles and select point analysis results.

The results for the A/V/G specimen showed that the layers were of high purity (AES has an elemental sensitivity of 0.1%). However, V and O Auger peaks were in the scan electron energy range and would overlap making it difficult to resolve whether or not O was present in the V layer. The AES results showed that the heat treatments (as seen for A/V/PP) induced aluminum, carbon and oxygen diffusion. Oxygen was in a higher concentration in the aluminum layer as opposed to the other regions, seen qualitatively in Fig. 9b, and from concentration calculations. This result might suggest that oxygen was a product of the heat treatment process, except that the heat treatments were conducted in flowing argon which had an in-line oxygen scrubber, in a similar manner to that reported elsewhere [1, 5, 8]. Select point analysis showed a very small Al AES peak to be present beyond the depth profiling once the graphite substrate was reached. Oxygen activity was observed in that the O and V profiles did not stay proportional in the profiles for the heat treated specimens as they were for the deposited cases. Oxygen was most likely to be from the graphite, since the substrates contained an unknown amount of residual oxygen. Carbon showed up in the vanadium layer at a higher concentration for the A/V/PA specimen when compared to the A/V/PP one indicating that it diffused more readily with this substrate orientation.

3.3. Discussion

The complexity of the interfaces in composite materials is seen in this research, even though the model interfacial system started out having a single interfacial layer of high purity. The ability to experimentally separate the interfacial system into Al/V and V with Al and C boundaries, where interface interactions were observed from the vantage point of the V, lead to results which were otherwise not obtainable. It was observed that upon formation of the Al/V interface couple, the interface started out with some in-

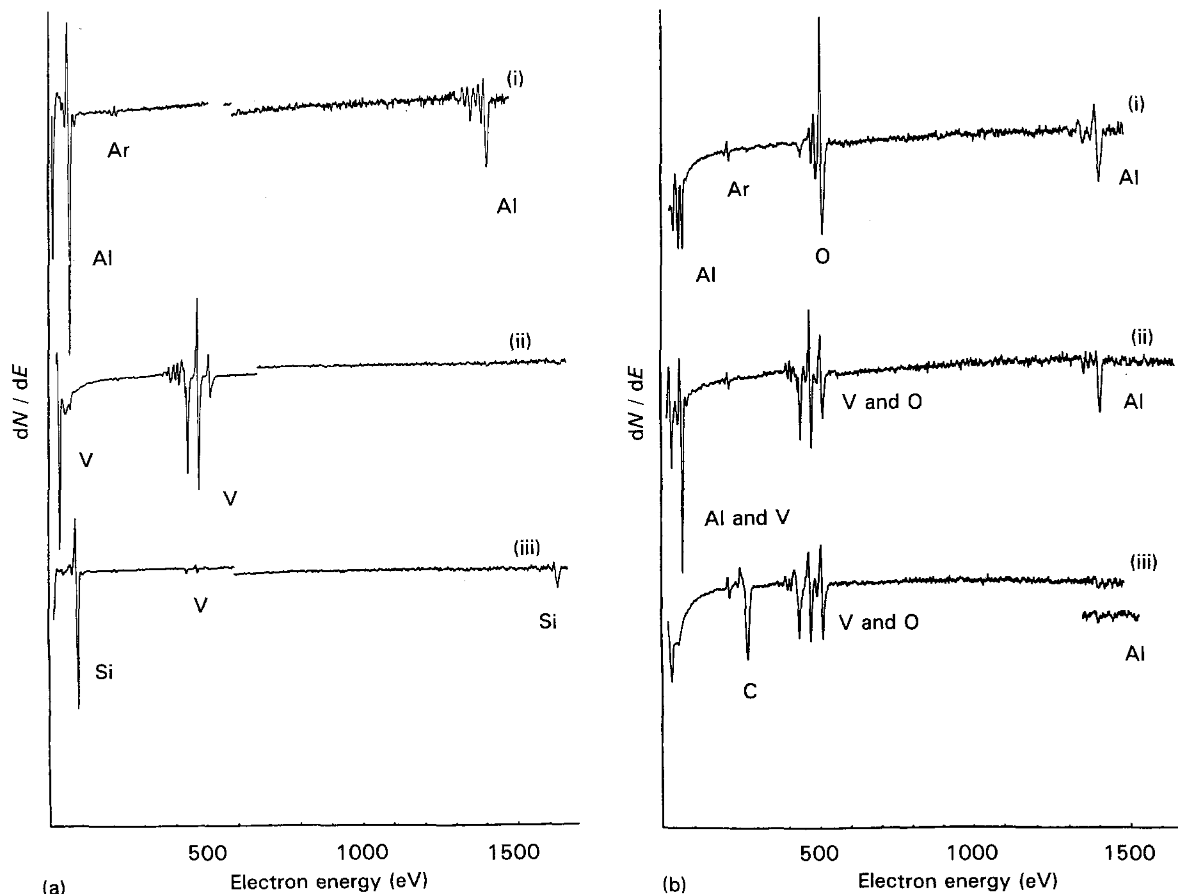

Figure 9 Select point analysis for (a) the A/V/S showing the Al layer (i), V layer (ii), and V/Si interface (iii) and (b) the A/V/PP heat treated for 40 min showing the Al layer with oxygen (i), V diffusion layer (ii), and V/C interface (iii). The repeat scan of Al was run to verify the presence of Al.

herent roughness even though smooth substrates were used as well as cooled. The intermixing was not extensive and it was not until a temperature of 325 °C was reached and maintained for 10 min that extended reactions occurred. Other investigations of Al-transition metal interface systems have shown that the Al-rich phases form first and that the presence of other Al/metal phases is dependent on the kinetics of the reaction and the processing method, therefore Al_3V was expected to form [4, 5, 8–10]. The Al_3V had a tetragonal $D0_{22}$ structure similar to Al_3Ti, used in this research as a standard. Research on Al–Ti intermetallics by Maruyama *et al.* [11] showed that the first phase to form in an Al–Ti couple is Al_3Ti. In bulk interdiffusion couples a number of phases can be present, whereas in interface couples formed by deposition methods, as in the semiconductor industry, single phases can occur or more than one phase can be formed dependent on the processing conditions. The reactions that occurred in the Al/V interface were significant in that the control of the growth of these phases could lead to well-tailored interfaces [12].

A comprehensive XAFS study using small angle XAFS and glancing angle XAFS showed that at low temperatures Al–V interactions were by phase formation of Al_3V, however, this phase formation did not dominate at higher temperatures. Instead, interdiffusion of Al, C and O occurred where the V never fully reacted employing the processing parameters used in this study. The decrease in amplitude of the $k\chi(k)$ data and the reduction in the height of the peaks on the M/T indicated that intermixing with no extensive reaction occurred at temperatures as low as 300 °C. Reactions were not observed until the specimens were heat treated at 500 °C where the most likely interaction which dominated was the V–O interaction. Comparisons with the standards beyond that of V foil were not as easy but can be described as changes in $\chi(k)$ at low k, associated with oxide formation which occurred for both the A/V/PA and A/V/PP specimens–oxidation of the V layer was more pronounced in the A/V/PP specimen. Oxygen, like Al and C, diffused extensively and reactions were not seen to occur until high temperatures were reached.

The AES results (both select point analysis and depth profiling) confirmed that oxygen diffused throughout the A/V/PP specimen to a greater extent than in the A/V/PA specimen. Carbon was found in the Al region for both specimens, more pronounced for the A/V/PA following the 500 °C heat treatment, yet the XAFS still indicated the interaction of V with an element which would produce a peak in the M/T at ~ 0.15 nm. The AES data for the 500 °C heat treated specimens also showed that Al diffused to the graphite substrate, a result that could not be observed using XAFS. Although Al diffusion to the graphite is not desired it is not a true indication that this would occur at a service temperature of 300 °C.

4. Conclusions

This research investigated the high temperature interactions of a model Al/V/graphite composite interfacial system. It was observed that there was a temperature below which no interactions in the interface occurred (325 °C for this system) and that once that temperature was exceeded the interactions in the interface varied dependent on the temperature of the system. These results suggest that XAFS is a very good tool for composite interface studies of this type and would provide useful data to control the interface microstructure of composite materials. A better understanding was also obtained as to the formation of Al-rich intermetallic phases in that even though they formed at low temperatures, they would not necessarily progress as the temperature of the composite processing is raised. The high temperature interactions of this interface couple seem to indicate that V would not act as a useful diffusion barrier to replace titanium diboride, since diffusion occurred and *in situ* phases of interest (those of Al_3Ti and VC) which might otherwise slow down diffusion, were not extensively formed without proper control.

Acknowledgements

The authors would like to acknowledge the many helpful discussions with S. M. Heald at Brookhaven National Laboratory and B. Maruyama at Wright Patterson Air Force Base. Support for NSLS Beamline X-11A was provided by the US Department of Energy, Division of Materials Science under contract no. DE-AS05-80-ER10742. The authors also thank H. L. Marcus for use of the Scanning Auger Microprobe at The University of Texas at Austin.

References

1. R. D. MATHIS, Thin Film Evaporation Source Reference, R. D. Mathis cat., (R. D. Mathis Co., Long Beach, CA, 1993).
2. E. V. BARRERA, BENJI MARUYAMA and J. E. BENCI, *Adv. Compos. Mater., Ceram. Trans.* **19** (1991) 1035.
3. BENJI MARUYAMA, E. V. BARRERA, R. K. EVERETT, W. M. HENSHAW and S. M. HEALD, in Proceedings on Controlled Interfaces in Composites, the 3rd International Conference on Composite Interfaces (ICCI-III), edited by H. Ishida (Elsevier, Amsterdam, 1990) p. 175.
4. L. G. PARRATT, *Phys. Rev.* **95** (1954) 359.
5. S. M. HEALD and J. M. TRANQUADA, in "Physical methods of chemistry", edited by B. W. Rossiter and J. F. Hamilton (Wiley, New York, 1990) p. 189.
6. S. M. HEALD and E. V. BARRERA, *J. Mater. Res.* **6** (1991) 935.
7. G. E. BACON, "Neutron diffraction", 2nd Edn (Oxford University Press, London, 1962).
8. T. T. MICKLE, E. V. BARRERA, W. E. FRAZIER and J.E. TALIA, in Proceedings of the Symposium on Melt Spinning, edited by E. F. Matthys (TMS, San Diego, CA, 1992) p. 183.
9. H. CHEN and S. M. HEALD, *J. Appl. Phys.* **66** (1989) 1793.
10. H. CHEN, PhD thesis, City University of New York, New York, USA (1989).
11. BENJI MARUYAMA, F. S. OHUCHI and L. RABENBERG, *J. Mater. Sci. Lett.* **9** (1990) 864.
12. J. E. TALIA, T. T. MICKLE, W. E. FRAZIER and E. V. BARRERA, in Proceedings on Developments in Ceramic and Metal Matrix Composites, edited by K. Upadhya (TMS, San Diego, CA, 1992) p. 157.
13. S. U. CAMPISANO, G. FOTI, E. RIMINI, S. S. LAU and J. W. MAYER, *Phil. Mag.* **31** (1975) 903.

Received 11 June 1993
and accepted 28 February 1994